NOTES AND CORRESPONDENCE

Application of the Eliassen Balanced Model to Real-Data Tropical Cyclones

JOHN MOLINARI, DAVID VOLLARO, AND STEVEN SKUBIS

Department of Atmospheric Science, State University of New York at Albany, Albany, New York

29 July 1992 and 29 January 1993

ABSTRACT

The Eliassen balanced vortex model assumes gradient balance of the azimuthal mean flow. This assumption was tested by calculating mean and eddy terms in the radial momentum equation in the synoptic-scale environments of two tropical cyclones. The azimuthally averaged gradient balance was accurate to within 15%–25% in the free atmosphere outside the core, even in the asymmetric outflow layer. Balanced secondary circulations correlated well with circulations that included gradient thermal wind imbalance terms. Although the balanced model lacks Galilean invariance, balanced circulations were largely insensitive to use of a fixed coordinate or a coordinate moving with the storm. This occurred because changes in eddy heat and angular momentum fluxes largely offset one another. The two-dimensional balanced solutions provide a reasonably robust measure of circulations induced by azimuthal eddy processes in the tropical cyclone environment.

Nevertheless, individual forcing functions, such as the commonly examined lateral eddy flux convergence of angular momentum, often varied enormously between fixed and moving coordinates. Logic and available evidence suggest that such terms are meaningful only in a coordinate system moving with the storm.

1. Introduction

Eliassen (1952) investigated the response of an axially symmetric vortex in gradient balance to heat and momentum sources. Such two-dimensional balanced models have proven quite useful in understanding symmetric dynamics and thermodynamics in the tropical cyclone core (Ooyama 1969; Sundqvist 1970; Willoughby 1979; Smith 1981; Shapiro and Willoughby 1982; Schubert and Hack 1983; Emanuel 1989). Subsequent primitive equation simulations of isolated tropical cyclones largely confirmed the results of the two-dimensional balanced models (Ooyama 1982). Tropical cyclones in nature, however, are often highly asymmetric, particularly in the upper troposphere outside of the core. The role of azimuthal eddies in the dynamics must also be considered. A prognostic version of the two-dimensional Eliassen model was extended by Pfeffer and Challa (1981) to include lateral fluxes of angular momentum by azimuthal eddies. They showed that such fluxes—time invariant and specified from an observed composite of intensifying tropical cyclones—produced enhanced radial–vertical circulation that deepened the model storm to hurricane intensity. When the fluxes were removed, no intensification occurred. The results suggested that azimuthal asymmetries have significant influences on tropical cyclones in nature.

Corresponding author address: Prof. John Molinari, Department of Meteorology, State University of New York at Albany, Earth Science 225, Albany, NY 12222.

Molinari and Vollaro (1990), Molinari (1993), and Alsheimer (1992) have used a diagnostic version of the two-dimensional Eliassen model that includes not just lateral momentum fluxes but all eddy terms in the tangential momentum and thermodynamic equations, consistent with the scaling of Craig (1991). They constructed time series of the balanced adiabatic response to such fluxes. A remarkable sequence of events occurred in each of the three storms studied (Elena 1985, Allen 1980, and Danny 1985). A tropical cyclone approached an upper-tropospheric positive potential vorticity anomaly, and the balanced solution showed an upward motion maximum approaching the core. The upward motion was associated with both heat and momentum fluxes, but the latter dominated. The vertical circulation can also be viewed as associated with upper-tropospheric potential vorticity advection. When the induced upward motion reached the tropical cyclone core, a secondary eyewall (in Danny, the initial, primary eyewall) developed. The contraction of this feature coincided with dramatic intensification. The time series of balanced circulations thus had considerable value in diagnosing the interactions of the tropical cyclones with the upper vorticity sources. In addition, the balanced circulations showed features that were not present in the divergent flow in the operational analyses, due to the many distortions of small-scale divergence fields present in the operational procedures for analysis, adiabatic initialization, and diabatic initialization (Molinari et al. 1992). In terms of the divergent circulation, the two-dimensional balanced solutions were more useful than those based on the operational full-physics primitive equation model.

Overall, there is little question that the two-dimensional balanced model has been of considerable value in hurricane studies. In the application of this model, however, several issues have been overlooked (by the current authors as well) that involve the application of idealized models to real-data cases. First, of course, is whether azimuthally averaged gradient balance actually holds to a reasonable degree on the scale of the calculations. As will be discussed later, the extent of azimuthally averaged gradient balance can in principle differ significantly from the extent of local gradient balance. In the Eliassen model, it is the local time derivative of gradient thermal wind imbalance that is neglected, so that imbalances can be allowed if their time change is small. Solutions have not previously been calculated that include the nongradient balance terms to test the sensitivity to the balance assumption. Finally, the Eliassen model solution is not Galilean invariant: the assumption of balance has previously been made both in a fixed coordinate (Pfeffer and Challa 1981) and in a coordinate moving with the system (Molinari and Vollaro 1990). Logic suggests that the moving coordinate should be used, but no evaluation has been carried out.

The current note will address these complications of applying the idealized balance model to real-data cases. Because the European Centre for Medium-Range Weather Forecasts (ECMWF) operational analyses will be used, the results will apply not to the tropical cyclone core but rather to balanced circulations induced by resolvable features in the tropical cyclone environment. Such questions as, for example, whether tropical cyclone intensification is a balanced process cannot be addressed. Rather, the goal is to evaluate the robustness of previous two-dimensional balanced solutions with regard to the issues raised in this section.

2. Data sources

This study made use of ECMWF gridded analyses containing 2.5° horizontal resolution at seven mandatory levels in the vertical (1000, 850, 700, 500, 300, 200, and 100 mb). These analyses were bilinearly interpolated to cylindrical coordinates centered on the tropical cyclone position at each observation time, using 25-km radial grid spacing, 5° azimuthal spacing, and 25-mb vertical spacing, similar to Molinari and Vollaro (1990).

Hurricanes Elena of 1985 and Allen of 1980 were examined. Molinari et al. (1992) compared ECMWF analyses of the outflow layer of these storms to objective analyses of the same region. The latter used specialized datasets containing extensive upper-level cloud-motion vectors and were used to represent the true state of the atmosphere. In general, ECMWF analyses accurately represented the azimuthally averaged nondivergent flow but, as noted earlier, poorly represented azimuthally averaged divergent flow. Fluxes by azimuthal eddies were surprisingly robust outside the storm core, largely because such eddies represent balanced features in the tropical cyclone environment. Molinari et al. (1992) provide further details.

3. Evaluation of gradient balance

A necessary (and, along with hydrostatic balance, sufficient) assumption for the validity of Eliassen's (1952) balanced vortex equation is

$$\frac{\bar{v}_L^2}{r} + f_0\bar{v} + g\frac{\partial \bar{z}}{\partial r} = 0, \tag{1}$$

where v_L is storm-relative tangential velocity, r is radius, the bar indicates an azimuthal average, and f_0 is the Coriolis parameter at the storm center. Because $\bar{v}_L = \bar{v}$, (1) is identical in fixed and storm-relative coordinates.

The nature of the azimuthally averaged gradient balance in (1) can be seen in the following. Assume that (i) a large-amplitude midlatitude trough exists northwest of a tropical cyclone, and (ii) the flow at each point is close to (local) gradient balance, so that $(v^2/r_T) + fv + g(\partial z/\partial n) = 0$, where r_T is the local radius of trajectory curvature and n is normal to and left of the wind direction. It is quite possible that in this flow, which is everywhere close to gradient balance, the azimuthally averaged flow is *not* in gradient balance, because the flow in the trough is producing significant advection of radial momentum (for instance, via the term $-\overline{u'\partial u'/\partial r}$).

To address whether azimuthally averaged gradient balance holds, the full equation for the azimuthally averaged radial component of the motion must be evaluated. This equation is given in a coordinate moving with the storm by a rearrangement of (B13) in appendix B:

$$\frac{\bar{v}_L^2}{r} + f_0\bar{v} - g\frac{\partial \bar{z}}{\partial r} = \frac{\partial_L \bar{u}_L}{\partial t} + \frac{1}{r}\frac{\partial}{\partial r}(r\bar{u}_L^2) + \frac{\partial}{\partial p}(\bar{u}_L\bar{\omega}) + \frac{\overline{u_L'^2}}{r} + \frac{\partial}{\partial r}(\overline{u_L'^2}) + \frac{\partial}{\partial p}(\overline{u_L'\omega'}) - \frac{\overline{v_L'^2}}{r} - \overline{f'v'} + \Gamma, \tag{2a}$$

where, following Holland (1983),

$$\frac{\partial_L}{\partial t} = \frac{\partial}{\partial t} + \mathbf{v}_c\cdot\nabla, \tag{2b}$$

and $\mathbf{v}_c$ is the storm-motion vector. In real-data calculations, the right-hand side of equations does not equal the left-hand side, due to truncation errors in time and space, and sampling, measurement, and analysis errors. The term Γ has been added to (2a) to represent these errors plus the effects of friction, which are difficult to evaluate accurately. The right-hand side of (2a) shows the terms neglected by the assumption of gradient balance of the azimuthal mean flow. The mean magnitude

of each term in (2a) will be calculated, averaged over pressure and time for each radius, and over radius and time for each pressure level. The results can be interpreted as a scaling of terms for real-data cases. For reasons discussed in appendix A, the $\overline{u_L'^2}/r$ and $\overline{v_L'^2}/r$ terms must be combined for the scaling to be meaningful. To measure the overall gradient imbalance, the mean magnitude of the sum of the three left-hand-side terms will be computed as well.

Figures 1a and 1b show for Hurricanes Elena and Allen, the radial variation of the mean magnitudes of each of the three gradient balance terms, the sum of the three terms, the eddy Coriolis term (essentially a β effect), the term $\partial/\partial r(\overline{u'^2})$, and the residual Γ, each averaged over pressure and time. All the remaining right-hand-side terms were small: the term $(\overline{u_L'^2}/r) - (\overline{v_L'^2}/r)$ is shown in appendix A, while the mean and eddy vertical flux convergence terms, the mean lateral flux convergence term, and the Lagrangian time change term each were less than 2×10^{-5} m s^{-2} at all radii in both storms.

In Elena, the three terms that make up gradient balance of the azimuthal mean flow dominated at all radii. The mean centrifugal force term became negligible outside of the 800-km radius, and geostrophic balance held thereafter. The nongradient balance terms did not exceed 15% of the largest terms, except at radii outside about 1800 km. In this region, the β effect became noticeable, so that even geostrophic balance of the azimuthal mean was disrupted. Nevertheless, this effect was small within 2000 km of the center.

Figure 1b shows the same fields for Allen. Unlike Elena, Allen experienced no large-amplitude midlatitude wave passages during its life cycle. The magnitudes of all terms were generally smaller, but nongradient balance terms remained relatively unimportant.

The magnitude of the sum of the three left-hand-side terms in (2a) provides a more rigorous test of gradient balance, but one more subject to truncation error. Figure 1 shows that outside of the 100-km radius, the gradient deviation term amounted to less than 30% of the largest terms for both storms. At radii inside of 100 km, however, the imbalance became significant. These imbalances almost certainly arose because height and wind were independently interpolated from global analyses, and the resulting fields cannot describe the inner structure of the storms. Thus, as noted earlier, whether imbalances exist in the tropical cyclone core cannot be addressed by this study. Nevertheless, such presumably spurious imbalances may influence the robustness of the balanced solutions and thus cannot be ignored. This issue will be examined in the following section.

Figure 2 shows the three gradient balance terms and their sum, averaged over radius and time as a function of pressure. Gradient balance of the azimuthal mean was a good approximation except where friction disrupted it near the surface. Of note is the relatively small imbalance at 200 mb, the level in tropical cyclones where asymmetries typically have the greatest magnitude.

The magnitude of the residual Γ supports the previous reasoning. At inner radii and in the planetary boundary layer, almost all of the left-hand-side imbalances are represented by Γ. This indicates that these imbalances are related to the presence of friction and/

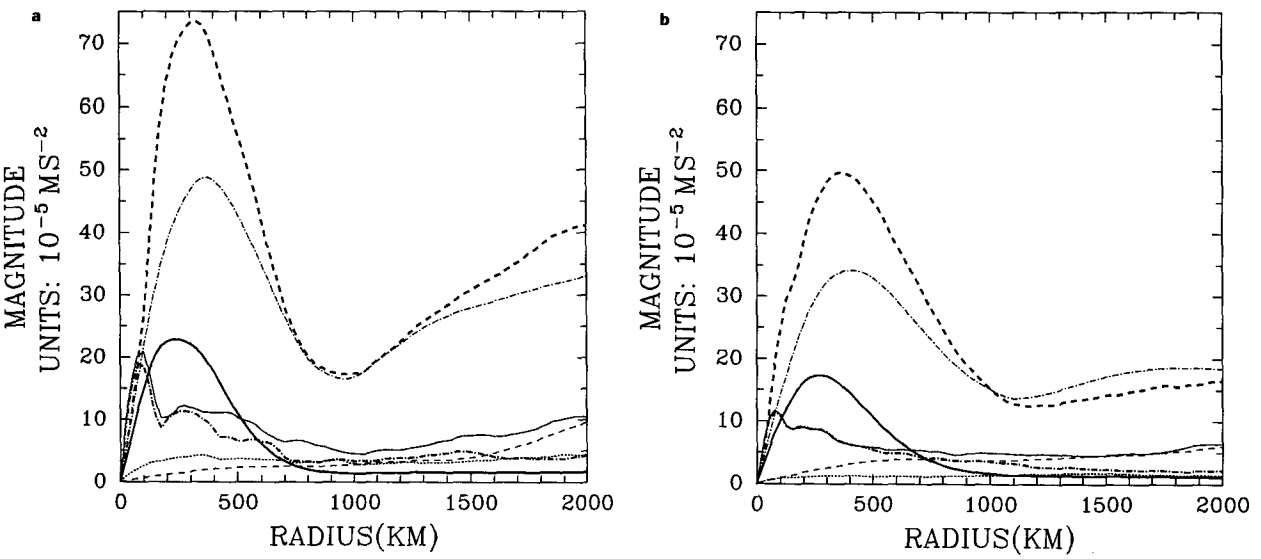

FIG. 1. Mean magnitude of terms in the radial momentum equation [Eq. (2a); units: 10^{-5} m s^{-2}], averaged over time and pressure for (a) Hurricane Elena and (b) Hurricane Allen. Shown are pressure gradient force (heavy dashes), Coriolis and centrifugal forces from the mean flow [$f_0\bar{v}$ (dash–dot) and $\bar{v}^2/r$ (heavy solid), respectively], the β-effect term $\overline{f'v'}$ (light dashes), the term $-\partial/\partial r(\overline{u'^2})$ (dotted), the sum of the three left-hand-side terms (light solid), and the variable Γ (dark dash–dot). The mean and eddy vertical flux terms and the time tendency $\partial_L\bar{u}_L/\partial t$ are less than 2×10^{-5} m s^{-2} at all radii and are not shown. The small term $(\overline{u_L'^2}/r - \overline{(v_L'^2}/r)$ is shown in Fig. A1.

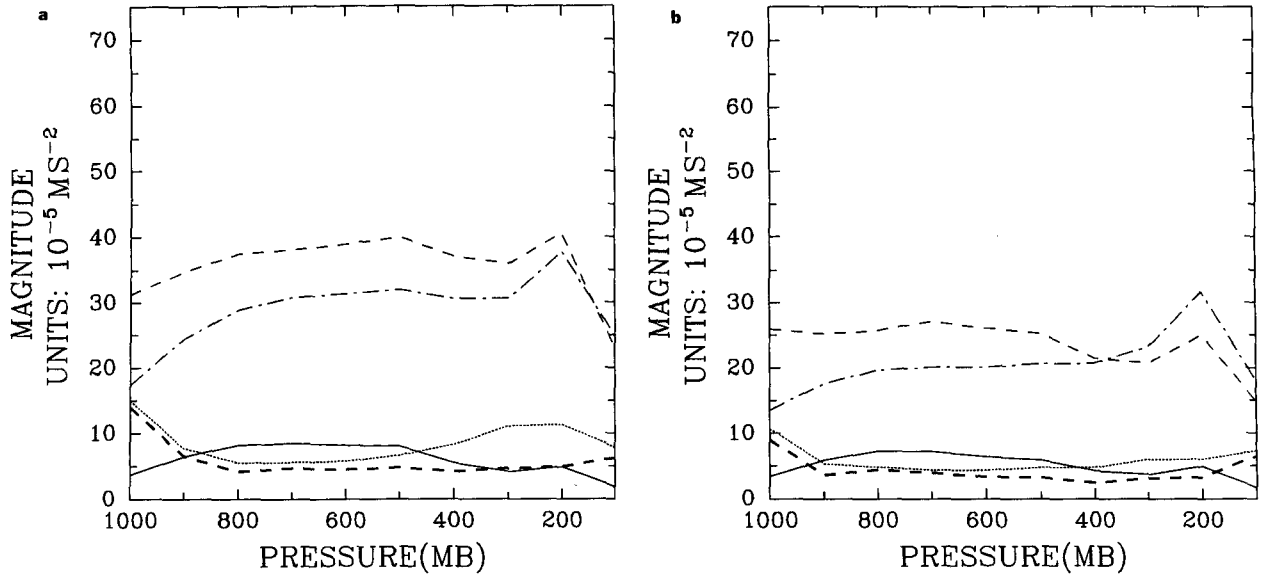

FIG. 2. As in Fig. 1 but averaged over radius and time for each pressure level. Shown are only five terms: pressure gradient force (light dashes), Coriolis and centrifugal forces from the mean flow (dash–dot and solid, respectively), the mean magnitude of the sum of the three (dotted), and the variable Γ (dark dashes).

or analysis and interpolation errors. At large radii and in the free atmosphere, Γ is very small. In these regions, calculated imbalances relate to physical processes represented by other right-hand-side terms, such as fluxes of radial momentum by eddies and the beta effect.

Figures 1 and 2 show that the regions of gradient imbalance occurred largely near the surface and at inner radii, which together represent a small fraction of storm volume. Subsequent sections will examine the sensitivity of the balanced circulations to these imbalances, and to the use of a moving coordinate.

4. Influences on balanced solutions

a. Fixed versus moving coordinate

The equation for the streamfunction representing the secondary circulation needed to maintain gradient balance can be written as

$$\mathcal{L}(\psi_1) = F_L, \tag{3}$$

where the second-order linear operator $\mathcal{L}$ (Sundqvist 1970) is given in appendix B. Following Molinari and Vollaro (1990), F_L represents eddy sources of angular momentum and potential temperature in a storm-following coordinate:

$$F_L = r\frac{\partial}{\partial p} \times\left[\left(\frac{2\bar{v}_L}{r}+f\right)\left(-\frac{1}{r^2}\frac{\partial}{\partial r}r^2\overline{u'_Lv'_L}-\frac{\partial}{\partial p}\overline{\omega'v'_L}-\overline{f'u'}\right)\right] + \frac{r\pi R}{c_pp}\frac{\partial}{\partial r}\left(-\frac{1}{r}\frac{\partial}{\partial r}r\overline{\theta'u'_L}-\frac{\partial}{\partial p}\overline{\theta'\omega'}\right), \tag{4a}$$

where

$$\pi = c_p\left(\frac{p}{p_0}\right)^{R/c_p} \tag{4b}$$

is the Exner function [π has been redefined from that used by Molinari and Vollaro (1990) to better represent standard symbolism]. As discussed by Molinari and Vollaro (1990), friction and heating were omitted from (4a) in order to isolate the adiabatic circulation associated with the eddy sources in the tropical cyclone environment. Accurate estimates of the diabatic term would in any event be difficult using global analyses. The streamfunction ψ_1 determines the divergent circulation required to maintain gradient balance in a cylindrical volume moving with the storm.

A second streamfunction defines the balanced response in the fixed coordinate (see appendix B):

$$\mathcal{L}(\psi_2) = F, \tag{5}$$

where F represents the eddy momentum and heat sources in the fixed system, given by

$$F = r\frac{\partial}{\partial p} \times\left[\left(\frac{2\bar{v}}{r}+f\right)\left(-\frac{1}{r^2}\frac{\partial}{\partial r}r^2\overline{u'v'}-\frac{\partial}{\partial p}\overline{\omega'v'}-\overline{f'u'}\right)\right] + \frac{r\pi R}{c_pp}\frac{\partial}{\partial r}\left(-\frac{1}{r}\frac{\partial}{\partial r}r\overline{\theta'u'}-\frac{\partial}{\partial p}\overline{\theta'\omega'}\right). \tag{6}$$

The left-hand-side operator in (5) does not change from the moving system because only mean-field derivatives are involved. The streamfunction ψ_2 determines the

divergent circulation required to maintain gradient balance in a fixed cylindrical volume centered on the instantaneous position of the storm.

The difference between ψ_1 and ψ_2 represents the influence of the moving coordinate on the balanced solution. Table 1 shows this difference using linear correlation coefficients between balanced $\bar{\omega}$ fields calculated from ψ_1 and ψ_2 at each observation time. (Streamfunction fields were not used directly because they contain an arbitrary constant.) Correlations were generally positive, but it is apparent that for rapid storm motion the fixed coordinate solution sometimes differed significantly (depending upon the degree of asymmetry in the environment). The mean linear correlation coefficients for storm speeds greater than 10, between 5 and 9.9, and less than 5 m s^{-1} were, respectively, 0.45, 0.67, and 0.96. The major differences occurred in the planetary boundary layer, and decreased rapidly with height. Figure 3 shows a time series of balanced $\bar{u}$ at 200 mb from the solutions to (3) and (5). Both qualitative and quantitative differences were quite small. In practice, it appears that using a moving or fixed coordinate should not matter greatly in the free atmosphere except for fast-moving storms in asymmetric environments.

TABLE 1. Linear correlation coefficients between balanced ω fields determined from fixed and storm-following coordinates [ω (ψ_1) vs ω (ψ_2)] and from balanced and unbalanced solutions [ω (ψ_1) vs ω (ψ_3)] for Hurricanes Elena (1985) and Allen (1980). Also shown is the speed of motion of the storms at each observation time.

Observation	Speed (m s^{-1})	ω (ψ_1) vs ω (ψ_2)	ω (ψ_1) vs ω (ψ_3)
Elena			
0000 UTC 28 August	12.9	0.52	0.91
1200 UTC 28 August	12.9	0.76	0.99
0000 UTC 29 August	8.6	0.80	0.91
1200 UTC 29 August	8.9	0.62	0.93
0000 UTC 30 August	4.9	0.92	0.98
1200 UTC 30 August	3.9	0.99	0.98
0000 UTC 31 August	2.7	0.99	0.99
1200 UTC 31 August	4.4	0.99	0.99
0000 UTC 1 September	0.0	1.00	0.98
1200 UTC 1 September	0.0	1.00	0.91
0000 UTC 2 September	3.4	0.98	0.96
1200 UTC 2 September	5.7	0.95	0.81
Allen			
0000 UTC 3 August	11.3	−0.13	0.44
1200 UTC 3 August	9.8	0.55	0.71
0000 UTC 4 August	9.0	0.76	0.77
1200 UTC 4 August	9.9	0.54	0.68
0000 UTC 5 August	9.6	0.82	0.97
1200 UTC 5 August	9.6	0.71	0.97
0000 UTC 6 August	9.9	0.31	0.87
1200 UTC 6 August	11.1	0.66	0.91
0000 UTC 7 August	8.5	0.50	0.60
1200 UTC 7 August	7.6	0.78	0.88
0000 UTC 8 August	7.2	0.55	0.79
1200 UTC 8 August	6.7	0.42	0.61
0000 UTC 9 August	6.3	0.82	0.91
1200 UTC 9 August	4.5	0.84	0.91
0000 UTC 10 August	3.1	0.89	0.93
1200 UTC 10 August	5.1	0.85	0.93

A single term in the forcing for the balance equation (4a), involving the lateral eddy flux convergence of angular momentum $-1/r^2(\partial/\partial r)(r^2\overline{u'_L v'_L})$ has been associated with tropical cyclone intensity change by Pfeffer and Challa (1981), Molinari and Vollaro (1989, 1990), and DeMaria et al. (1993). Pfeffer and Challa (1981) calculated this term in a fixed coordinate (i.e., with u, v replacing u_L, v_L), while the latter researchers used a coordinate moving with the storm. The momentum flux term is often studied in isolation simply because available data does not allow heat flux terms to be calculated. It is thus relevant to examine the influence of the choice of coordinate on this single term.

Figure 4 shows a time series of the lateral eddy flux convergence of angular momentum (divided by r to give units of meters per second per day) at 200 mb in Hurricane Allen in the moving and fixed coordinate. The changes in this term far exceed those of the overall balanced solutions; the magnitude, the overall pattern, and even the sign often differ. Because the moving coordinate values (Fig. 4a) have been shown to be largely insensitive to errors in storm position and motion and to analysis method (Molinari et al. 1992), the large differences in the two fields cannot be attributed to analysis or interpolation errors. It cannot be stated that only the moving coordinate value in Fig. 4 is "correct," in that both calculations are accurate to within analysis error. Nevertheless, the authors believe logic suggests that individual balance equation terms should be calculated moving with the cyclone, not in a fixed coordinate dominated by the motion of the cyclone out of the region. Support for this view is provided by the positive correlations between moving coordinate eddy momentum fluxes and intensity change in tropical cyclones by Molinari and Vollaro (1989) and DeMaria et al. (1993). In addition, Skubis and Molinari (1987) found that a moving coordinate angular momentum budget matched observed changes in Hurricane Eloise (1975) far better than a fixed coordinate. The fixed coordinate lateral momentum flux forcing from the composite hurricane used in a prognostic balanced model by Pfeffer and Challa (1981) might be suitable only due to the slow forward motion implied by the composite storm. It is apparent from Fig. 4 that when individual forcing functions are evaluated in fairly rapidly moving storms, the choice of a coordinate system cannot be taken lightly.

Changes in the overall balanced solutions are much smaller than those in the individual forcing functions because momentum flux convergence changes are substantially offset by changes of opposite sign in heat flux convergence, if mass and momentum are near balance. Appendix C shows an example of overlapping terms in the eddy momentum and heat flux expressions under geostrophic balance.

In summary, individual eddy forcing functions can vary enormously in fixed and moving coordinates, but

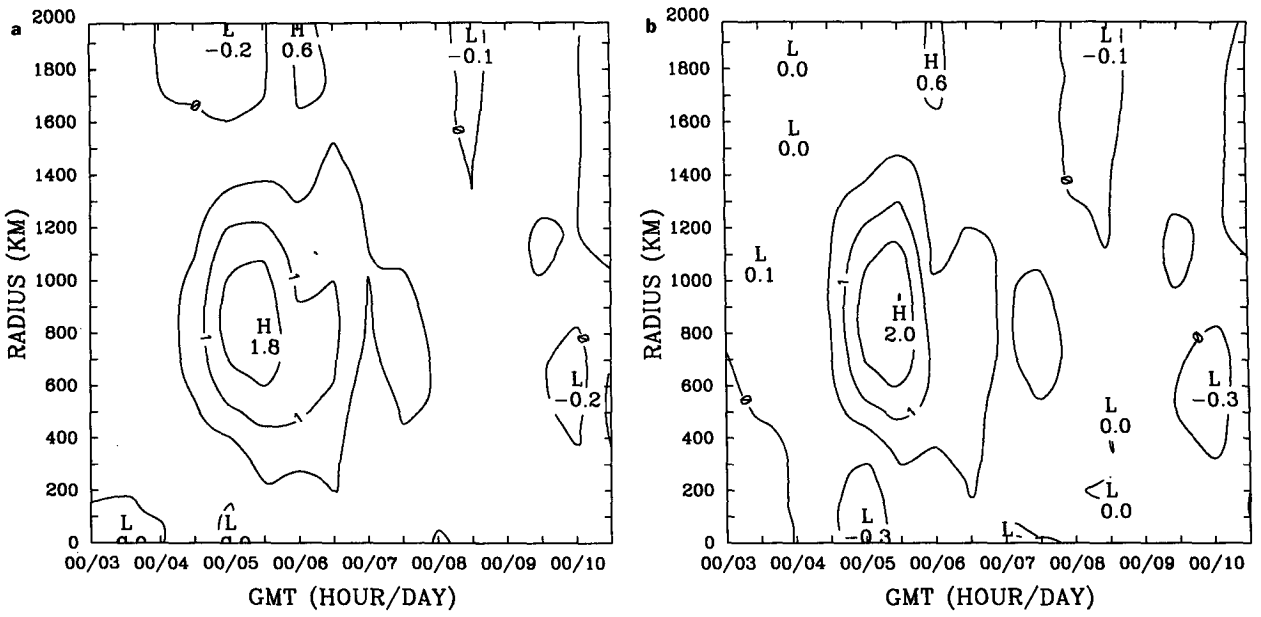

FIG. 3. Time series of the balanced radial component of the motion at 200 mb in Hurricane Allen, computed from the streamfunction in (a) the moving coordinate [Eq. (3)] and (b) the fixed coordinate [Eq. (5)]. Increment: 0.5 m s^{-1}.

balanced solutions vary by much less, with differences significant only for rapidly moving storms. Near the high-speed core of tropical cyclones, the changes in fixed and moving coordinate solutions might be larger. The results of this note apply only to balanced circulations in the tropical cyclone environment.

b. Influence of gradient thermal wind imbalances

In principle, gradient wind imbalances are allowed by the Eliassen system if the local time change of the gradient thermal wind imbalance is small. The difference in balanced solutions between fixed and moving systems occurs because the local time derivative differs in Eulerian and storm-following coordinates (see, for instance, Davies-Jones 1991). A third streamfunction is defined below to include the gradient thermal wind imbalance term in the moving coordinate (see appendix B):

$$\mathcal{L}(\psi_3) = F_L + r\frac{\partial_L}{\partial t}\left(\frac{\partial \bar{Z}_L}{\partial p}\right), \tag{7}$$

where $\bar{Z}_L$ is the gradient imbalance given by the sum of the three left-hand-side terms in (2a) and $\partial\bar{Z}_L/\partial p$ is the gradient thermal wind imbalance. The ψ_3 field represents an unbalanced streamfunction. The difference between ψ_1 and ψ_3 measures the influence on the solutions of the time change of gradient thermal wind imbalance in the moving coordinate. Table 1 shows generally large positive correlations between $\bar{\omega}$ fields calculated from ψ_1 and ψ_3, with a mean correlation of 0.87. The greatest differences occur at low levels where gradient imbalances are greatest. Figure 5 gives a time series of $\bar{u}$ at 200 mb in Hurricane Allen determined from ψ_3. Comparison to Fig. 3 shows that the upper-tropospheric differences in the balanced and unbalanced radial velocities are quite small.

The unbalanced streamfunction in the fixed coordinate is given (see appendix B) by

$$\mathcal{L}(\psi_4) = F + r\frac{\partial}{\partial t}\left(\frac{\partial \bar{Z}}{\partial p}\right). \tag{8}$$

The second right-hand-side term in (8) represents the Eulerian change of the gradient thermal wind imbalance. The value of $\bar{Z}$ (which equals $\bar{Z}_L$ because the two cylindrical coordinates share the same center position at each calculation time), is given by the sum of the three left-hand-side terms in (2a). It can be shown that ψ_3 should equal ψ_4. In addition, for a rapidly moving storm, negligible gradient thermal wind imbalances are unlikely to simultaneously occur in both the fixed and moving coordinates. Unfortunately, the calculated ψ_4 violated both conditions: ψ_3 and ψ_4 differed by as much as the other ψ fields, and $\bar{\omega}$ from ψ_2 and ψ_4 correlated well, indicating apparent balance in the fixed coordinate. These errors almost certainly arose due to truncation error in the right-hand-side time derivatives of (7) and (8), despite the use of fourth-order finite differencing in time. Truncation error may have been especially large in (8), because the 12-h observations could not see the large time change associated with the movement of the hurricane out of the fixed volume. It is likely that the balance assumption holds best in the moving coordinate, but the available data cannot confirm this.

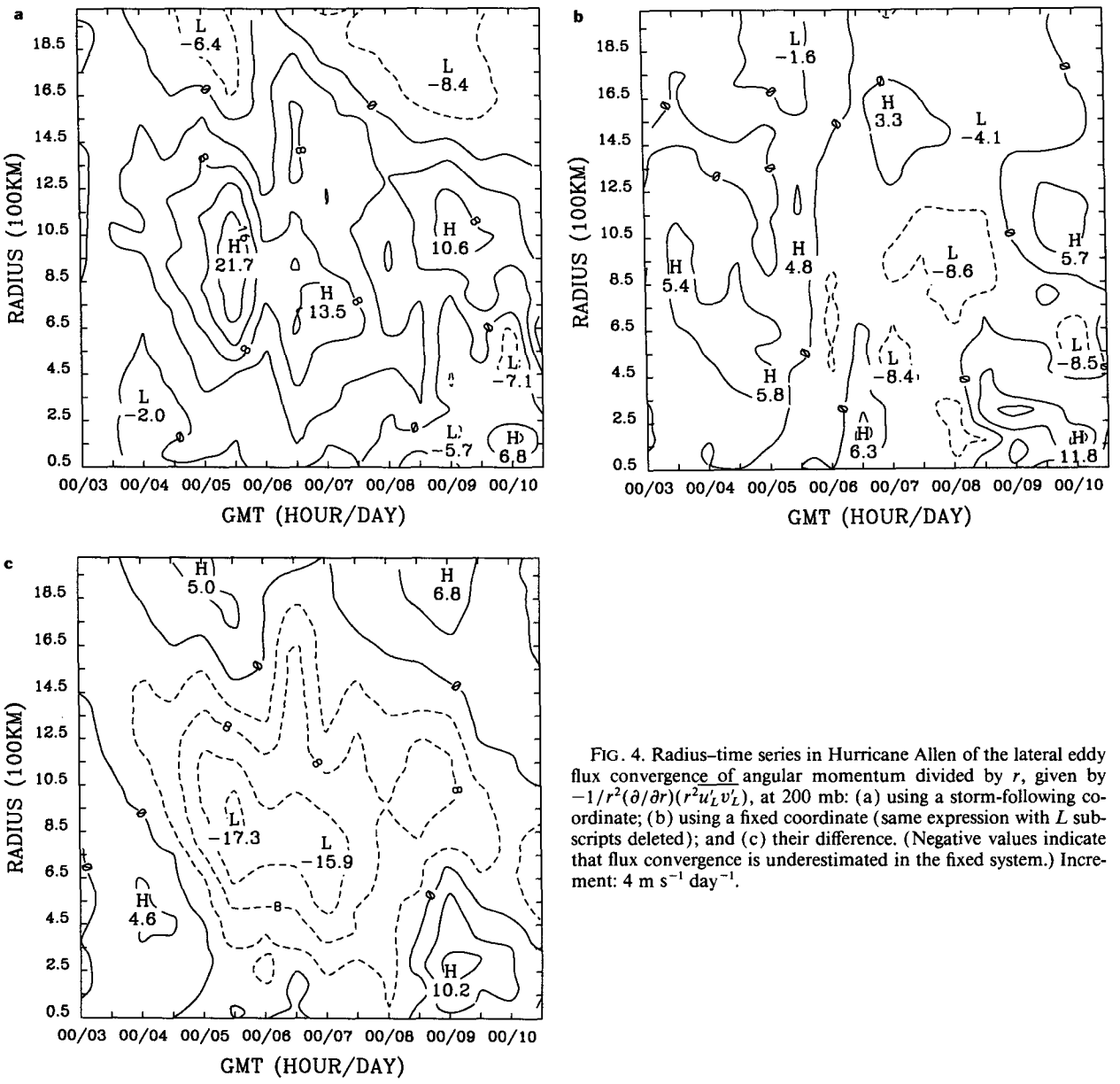

FIG. 4. Radius–time series in Hurricane Allen of the lateral eddy flux convergence of angular momentum divided by r, given by $-1/r^2(\partial/\partial r)(r^2u'_Lv'_L)$, at 200 mb: (a) using a storm-following coordinate; (b) using a fixed coordinate (same expression with L subscripts deleted); and (c) their difference. (Negative values indicate that flux convergence is underestimated in the fixed system.) Increment: 4 m s^{-1} day^{-1}.

5. Discussion and conclusions

The Eliassen balanced solution used in this paper averages out azimuthal variations. This is a significant weakness, because troughs approach from one side of the circulation, and asymmetric aspects of the interaction must also be understood. Recently, Raymond (1992) and Montgomery and Farrell (1993) have developed three-dimensional nonlinear balanced models. Although each has limitations on allowable flow structure and physical processes, it is likely that such models will have increasing value in studies of tropical cyclone interactions with their environment.

Nevertheless, the two-dimensional Eliassen balanced model has many benefits for studying the tropical cyclone environment in real-data studies. The azimuthal averaging makes calculation of the right-hand-side eddy flux terms quite robust (Molinari et al. 1992). Once azimuthal eddies are included, the basis for the model becomes the gradient balance of the azimuthal mean flow. This was shown to hold reasonably well outside of the boundary layer, even in the highly asymmetric outflow layer. To the extent that the local time change of the gradient thermal wind imbalance can be captured by 12-h data, the balance assumption appears sufficiently strong to justify use of the balanced equation.

Overall balanced solutions were quite similar in the fixed and moving coordinate, because large changes in heat and angular momentum flux terms partly cancelled, at least on the scales examined in this study.

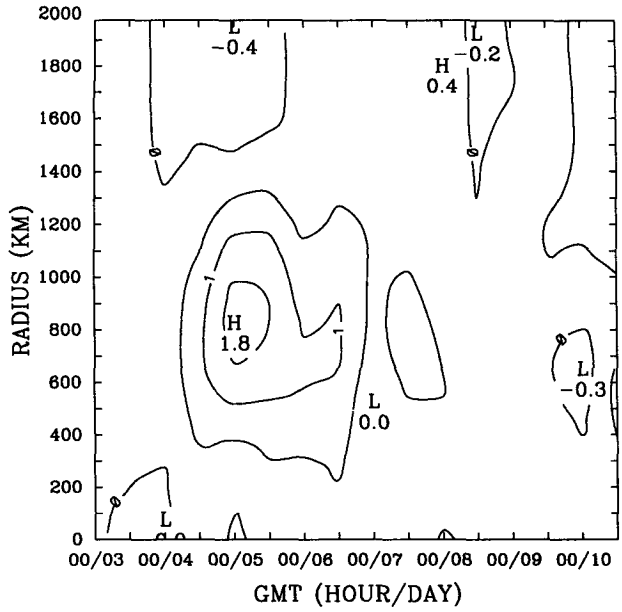

FIG. 5. As in Fig. 3 but determined from the unbalanced streamfunction [Eq. (7)].

For rapidly moving storms in asymmetric environments, however, the overall balanced solution may differ significantly, and the moving coordinate form (Molinari and Vollaro 1990) is most meaningful in such circumstances.

Due to data limitations, individual forcing functions from the balance equation involving eddy angular momentum sources are often considered in isolation. Such individual terms were shown to vary dramatically between a fixed coordinate and one moving with the storm. The evidence suggests that the isolation of individual balance equation terms involving eddy fluxes is meaningful only in the storm-relative framework provided by the moving coordinate.

Whereas prognostic balanced models may have initially small errors that accumulate with time, the results of this note suggest that a time series of diagnostic solutions each has small error. It has previously been argued that such a sequence (see Molinari and Vollaro 1990; Molinari 1993; Alsheimer 1992) provides insight into the process by which the synoptic-scale interacts with a tropical cyclone. The results of this work suggest that the two-dimensional Eliassen balanced solution is a reasonably robust tool for study of real-data tropical cyclone environments, even for rapidly moving or highly asymmetric storms.

Acknowledgments. We are indebted to Lloyd Shapiro of Hurricane Research Division (HRD) of NOAA for his cogent review of the manuscript. We thank Dr. Hugh Willoughby of HRD and Dr. David Knight of SUNYA for beneficial discussions during the course of the work. Gridded analyses were obtained from the European Centre for Medium-Range Weather Forecasts. This study was supported by the National Science Foundation through Grant ATM8902487.

APPENDIX A

Evaluation of Nonlinear Eddy Terms in the Radial Momentum Equation

Consider a uniform steady storm-relative flow across a tropical cyclone at a given level. It is intuitively clear that regardless of direction, such a flow is made up entirely of eddy components. Equation (2a) in the text has only two nonzero right-hand-side terms under such circumstances: $\overline{u_L'^2}/r$ and $-\overline{v_L'^2}/r$. These terms grow with decreasing radius as $1/r$, producing an apparent sharp deviation from gradient balance of the azimuthal mean. In reality, for the cylindrical coordinate transformation to be valid, the right-hand side of (2) must be zero for steady uniform flow. This occurs because the two nonzero terms exactly cancel for uniform flow across the storm.

Figure A1 confirms the importance of cross-storm relative flow in Hurricanes Elena and Allen. Shown are the mean magnitudes of the two eddy terms—averaged over pressure and time—the sum of the two terms, and a fourth curve representing either term for a 5 m s^{-1} uniform flow in any direction across the center. It is apparent that on average, a 5 m s^{-1} storm-relative flow occurred in each storm. Although both of these eddy terms are large at small radii due to storm-relative flow, their sum clearly is negligible versus the large terms shown in Fig. 1 of the text. Only the sum was included in the "scaling" in section 2.

One other consideration arises in the calculation of the right side of (2). To maintain vector invariance in the transformation from Cartesian to cylindrical coordinates, u' and v' must be nonzero and vary with azimuth at $r = 0$ (Shapiro and Willoughby 1991, personal communication). Their value comes straight from the transformation equations.

APPENDIX B

Equations in Storm-following Coordinates

The storm-relative flow vector is defined by

$$\mathbf{v}_L = \mathbf{v} - \mathbf{v}_c, \tag{B1}$$

where $\mathbf{v}_c$ is the storm-motion vector. Neglecting storm acceleration,

$$\frac{d\mathbf{v}}{dt} = \frac{d\mathbf{v}_L}{dt}. \tag{B2}$$

The horizontal frictionless equation of motion with pressure as a vertical coordinate can thus be written

$$\frac{d\mathbf{v}_L}{dt} = -f\mathbf{k} \times \mathbf{v} - g\nabla_p z. \tag{B3}$$

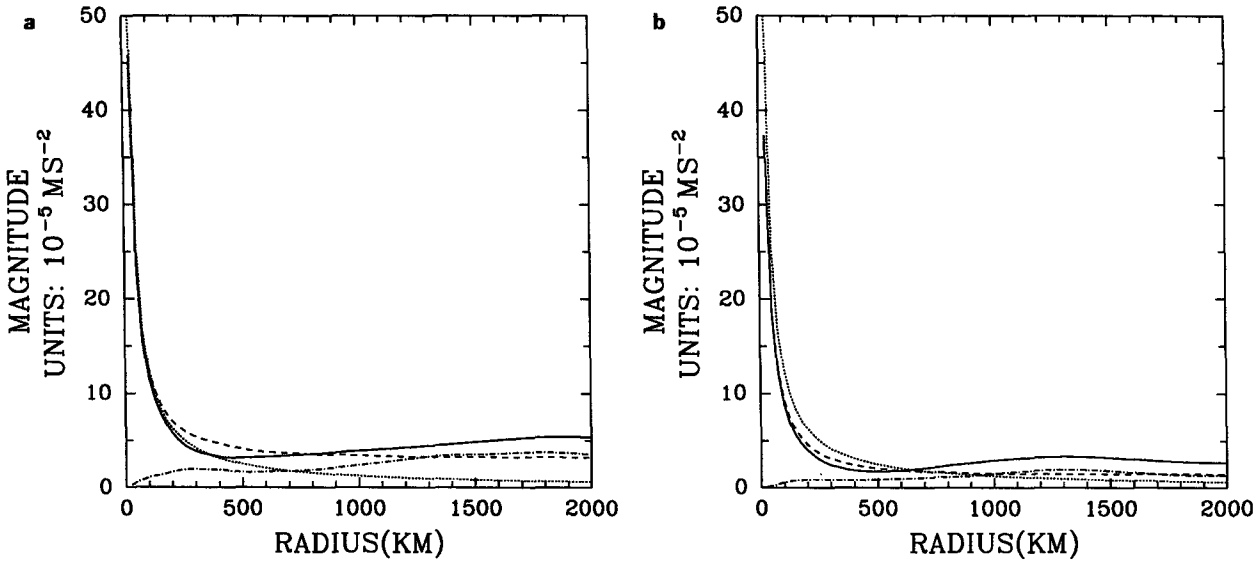

FIG. A1. Mean magnitudes, averaged over pressure and time, of two radial momentum equation terms—$-\overline{u_L'^2}/r$ (dashed) and $\overline{v_L'^2}/r$ (solid)—and their sum (dash-dot). Also shown is either term for a uniform 5 m s^{-1} flow across the storm (dotted): (a) Hurricane Elena and (b) Hurricane Allen.

The left-hand side of (B3) is given by

$$\frac{d\mathbf{v}_L}{dt} = \mathbf{i}_r \frac{du_L}{dt} + u_L \frac{d\mathbf{i}_r}{dt} + \mathbf{i}_\lambda \frac{dv_L}{dt} + v_L \frac{d\mathbf{i}_\lambda}{dt}, \quad \text{(B4)}$$

where u_L and v_L represent radial and tangential velocity, respectively. The total derivative will be expanded in a cylindrical coordinate moving with the storm, following Holland (1983):

$$\frac{d(\ )}{dt} = \frac{\partial_L(\ )}{\partial t} + \frac{1}{r}\frac{\partial r u_L(\ )}{\partial r} + \frac{1}{r}\frac{\partial v_L(\ )}{\partial \lambda} + \frac{\partial \omega(\ )}{\partial p}. \quad \text{(B5)}$$

It is straightforward to show that

$$\frac{d\mathbf{i}_r}{dt} = \frac{v_L}{r}\frac{\partial \mathbf{i}_r}{\partial \lambda} = \frac{v_L}{r}\mathbf{i}_\lambda \quad \text{(B6)}$$

$$\frac{d\mathbf{i}_\lambda}{dt} = -\frac{v_L}{r}\mathbf{i}_r. \quad \text{(B7)}$$

Thus, (B4) becomes

$$\frac{d\mathbf{v}_L}{dt} = \mathbf{i}_r\left(\frac{du_L}{dt} - \frac{v_L^2}{r}\right) + \mathbf{i}_\lambda\left(\frac{dv_L}{dt} + \frac{u_L v_L}{r}\right). \quad \text{(B8)}$$

Using (B8), the radial component of (B3) becomes

$$\frac{du_L}{dt} = \frac{v_L^2}{r} + fv - g\frac{\partial z}{\partial r}. \quad \text{(B9)}$$

Only the Coriolis term (and friction, if it were present) contains the total velocity field. Expanding the left-hand side of (B9) in the moving cylindrical system and rearranging gives

$$\frac{\partial_L u_L}{\partial t} = -\frac{1}{r}\frac{\partial}{\partial r}(ru_L^2) - \frac{1}{r}\frac{\partial}{\partial \lambda}(u_L v_L) - \frac{\partial}{\partial p}(u_L\omega) + \frac{v_L^2}{r} + fv - g\frac{\partial z}{\partial r}. \quad \text{(B10)}$$

Next, define

$$u_L(r, \lambda, p, t) = \bar{u}_L(r, p, t) + u_L'(r, \lambda, p, t) \quad \text{(B11a)}$$

$$v_L(r, \lambda, p, t) = \bar{v}_L(r, p, t) + v_L'(r, \lambda, p, t) \quad \text{(B11b)}$$

$$\omega(r, \lambda, p, t) = \bar{\omega}(r, p, t) + \omega'(r, \lambda, p, t) \quad \text{(B11c)}$$

$$f(r, \lambda) = f_0 + f'(r, \lambda), \quad \text{(B11d)}$$

where f_0 is the Coriolis parameter at the storm center and

$$\bar{(\ )} = \frac{1}{2\pi}\int_0^{2\pi}(\ )d\lambda. \quad \text{(B12)}$$

Substituting (B11) into (B10) and azimuthally averaging gives the final form of the equation for mean storm-relative radial velocity

$$\frac{\partial_L \bar{u}_L}{\partial t} = -\frac{1}{r}\frac{\partial}{\partial r}(r\bar{u}_L^2) - \frac{\partial}{\partial p}(\bar{u}_L\bar{\omega}) - \frac{1}{r}\frac{\partial}{\partial r}(r\overline{u_L'^2}) - \frac{\partial}{\partial p}(\overline{u_L'\omega'}) + \frac{\overline{v_L'^2}}{r} + \overline{f'v'} + \frac{\bar{v}_L^2}{r} + f_0\bar{v} - g\frac{\partial \bar{z}}{\partial r}. \quad \text{(B13)}$$

The right-hand-side terms represent, respectively, the lateral and vertical flux convergence of u_L by the mean flow, the lateral and vertical storm-relative eddy flux convergence, the eddy centrifugal and Coriolis accelerations, and the three terms comprising gradient balance of the azimuthally averaged flow.

Similarly, it can be shown that

$$\frac{\partial_L \bar{v}_L}{\partial t} = -\frac{1}{r^2}\frac{\partial}{\partial r}(r^2 \bar{u}_L \bar{v}_L) - \frac{\partial}{\partial p}(\bar{v}_L \bar{\omega}) - f_0 \bar{u} - \frac{1}{r^2}\frac{\partial}{\partial r}(r^2 \overline{u'_L v'_L}) - \frac{\partial}{\partial p}\overline{(v'_L \omega')} - \overline{f' u'} \quad \text{(B14)}$$

$$\frac{\partial_L \bar{\theta}}{\partial t} = -\frac{1}{r}\frac{\partial}{\partial r}(r\bar{\theta}\bar{u}_L) - \frac{\partial}{\partial p}(\bar{\theta}\bar{\omega}) - \frac{1}{r}\frac{\partial}{\partial r}(r\overline{\theta' u'_L}) - \frac{\partial}{\partial p}(\overline{\theta'\omega'}). \quad \text{(B15)}$$

The balance equation begins with the assumption of gradient balance of the azimuthally averaged flow [Eq. (1) in the text]. Taking the time derivative following the moving storm of the gradient thermal wind equation gives

$$\frac{\partial}{\partial p}\left[\left(\frac{2\bar{v}_L}{r} + f_0\right)\frac{\partial_L \bar{v}_L}{\partial t}\right] + \frac{R\pi}{c_p p}\frac{\partial}{\partial r}\left(\frac{\partial_L \bar{\theta}}{\partial t}\right) = 0, \quad \text{(B16)}$$

where $\partial_L/\partial t$ and π are given by (2B) and (4B), respectively, and the storm-following time change of f_0 associated with north–south storm motion has been neglected. Substituting (B14) and (B15) into (B16) and following the procedure described by Sundqvist (1970) gives the balance equation

$$\mathcal{L}(\psi_1) = F_L, \quad \text{(B17)}$$

where F_L, the eddy sources of θ and angular momentum, is given by (4), and

$$\mathcal{L}(\psi) = A\psi_{pp} + 2B\psi_{rp} + C\psi_{rr} - \frac{4B}{r}\psi_p - \left(\frac{1-\kappa}{p}B + \frac{C}{r}\right)\psi_r. \quad \text{(B18)}$$

Subscripts on ψ represent partial derivatives and

$$A = \left(f + \frac{2\bar{v}_L}{r}\right)\left(f + \frac{\partial \bar{v}_L}{\partial r} + \frac{\bar{v}_L}{r}\right) \quad \text{(B19)}$$

$$B = -\left(f + \frac{2\bar{v}_L}{r}\right)\frac{\partial \bar{v}_L}{\partial p} \quad \text{(B20)}$$

$$C = -\frac{R\pi}{c_p p}\frac{\partial \bar{\theta}}{\partial p}. \quad \text{(B21)}$$

In the fixed coordinate, the same procedure yields

$$\mathcal{L}(\psi_2) = F, \quad \text{(B22)}$$

where F is given by (6).

The full radial momentum equation in the moving coordinate is given by

$$\frac{\bar{v}_L^2}{r} + f_0\bar{v} + g\frac{\partial \bar{z}}{\partial r} = \bar{Z}_L, \quad \text{(B23)}$$

where $\bar{Z}_L$ represents the extent of azimuthally averaged gradient wind imbalance. The local time derivative (following the moving storm) of the thermal wind equation from (B23) yields

$$\frac{\partial}{\partial p}\left(\frac{2\bar{v}_L}{r} + f_0\right)\frac{\partial_L \bar{v}_L}{\partial t} + \frac{R\pi}{c_p p}\frac{\partial}{\partial r}\left(\frac{\partial_L \bar{\theta}}{\partial t}\right) = \frac{\partial}{\partial p}\left(\frac{\partial_L \bar{Z}_L}{\partial t}\right). \quad \text{(B24)}$$

Using the same procedure as earlier, but carrying the extra term, gives the following "balance" equation:

$$\mathcal{L}(\psi_3) = F_L + r\frac{\partial}{\partial p}\left(\frac{\partial_L \bar{Z}_L}{\partial t}\right). \quad \text{(B25)}$$

For the unbalanced fixed coordinate form, the procedure is similar, and the result is

$$\mathcal{L}(\psi_4) = F + r\frac{\partial}{\partial p}\left(\frac{\partial \bar{Z}}{\partial t}\right), \quad \text{(B26)}$$

where $\bar{Z} = \bar{Z}_L$, because (B23) is identical in fixed and moving coordinates.

In practice, cylindrical coordinate analyses from Molinari and Vollaro (1990) were centered on the storm at each analysis time, making $\partial_L/\partial t$ easy to compute by fourth-order finite differencing. To calculate $\partial/\partial t$ terms, 12-h cylindrical analyses were created, centered on a constant location (the storm position at the given time), and the same differencing was applied.

APPENDIX C

Influence of the Moving Coordinate on Balanced Solutions

Equations (4a) and (6) can be written, respectively, as

$$F_L = M_L + H_L$$
$$F = M + H, \quad \text{(C1)}$$

where M_L and M represent angular momentum source terms, and H_L and H represent heat source terms. The difference in the forcing term in the balance equation between moving and fixed coordinates is represented by $F_L - F$. Table 1 shows that the balanced solution does not change dramatically between the two coordinate systems, yet Fig. 4 shows that the momentum flux term (and the heat flux term, not shown) differs enormously. Thus, momentum and heat flux changes between fixed and moving systems must be offsetting one another; that is,

$$M_L - M \approx -(H_L - H). \quad \text{(C2)}$$

For this to be true there must be a large common term with opposite sign in the two expressions. Subtracting (6) from (4) and rearranging gives

$$F_L - F = \frac{\partial}{\partial p}\left[\frac{2\bar{v}}{r^2}\frac{\partial}{\partial r}r^2(\overline{u_c v} + \overline{u v_c})\right] + \frac{\partial}{\partial p}\left[(2\bar{v} + rf_0)\frac{\partial}{\partial p}(\overline{\omega v_c})\right] + \frac{\partial}{\partial p}\left[\frac{f_0}{r}\frac{\partial}{\partial r}r^2(\overline{u_c v} + \overline{u v_c})\right] + \frac{r\pi R}{c_p p}\frac{\partial}{\partial r}\left[\frac{1}{r}\frac{\partial}{\partial r}(r\overline{\theta u_c})\right], \quad \text{(C3)}$$

where u_c and v_c represent radial and tangential components of storm motion, respectively, and use has been made of the fact that $\overline{u_c} = \overline{v_c} = 0$, so that

$$\overline{\theta' u_c'} = \overline{\theta u_c}. \quad \text{(C4)}$$

Analogous expressions to (C4) exist for u, v, and ω when multiplied by a storm-motion component.

To show partial cancellation of momentum and heat flux terms in (C3) under the assumption of gradient balance has proven to be difficult owing to the complications of the bar operator on the nonlinear terms. Instead, v and θ are assumed to obey the geostrophic thermal wind balance:

$$\frac{\partial v}{\partial p} = -\frac{\pi R}{f c_p p}\frac{\partial \theta}{\partial r} \quad \text{(C5a)}$$

$$\frac{\partial u}{\partial p} = \frac{\pi R}{r f p c_p}\frac{\partial \theta}{\partial \lambda}. \quad \text{(C5b)}$$

Using (C5) and the following expressions (see Skubis and Molinari 1987),

$$\overline{\frac{v_c}{r}\frac{\partial \theta}{\partial \lambda}} = \frac{\overline{u_c \theta}}{r} \quad \text{(C6a)}$$

$$\overline{\frac{v_c}{r}\frac{\partial v}{\partial \lambda}} = \frac{\overline{u_c v}}{r} \quad \text{(C6b)}$$

gives

$$\frac{\partial}{\partial p}\left[\frac{f_0}{r}\frac{\partial}{\partial r}r^2(\overline{u_c v} + \overline{u v_c})\right] = -\frac{r\pi R}{c_p p}\frac{\partial}{\partial r}\left[\frac{1}{r}\frac{\partial}{\partial r}(r\overline{\theta u_c})\right]. \quad \text{(C7)}$$

As a result, the assumption of geostrophic balance produces a cancellation of the last two terms in (C3). This supports (but does not formally prove) the earlier result that the Eliassen balanced solutions in the Eulerian and storm-following coordinates differ by less than either of the forcing functions individually because changes in heat and angular momentum fluxes partially offset. Owing to the lack of Galilean invariance of the system, the two solutions would not be exactly equal in practice. As noted in the text, the offsetting of terms might not apply to the high-speed tropical cyclone core, where the coordinate-dependent curvature term is dominant.

REFERENCES

Alsheimer, Frank, 1992: Environmental interactions and inner core response during the development of Hurricane Danny. M.S. thesis, Department of Atmospheric Science, State University of New York at Albany, 62 pp. [Available from John Molinari, Department of Atmospheric Science, ES-225, State University of New York at Albany, 1400 Washington Avenue, Albany, NY 12222.]

Craig, G. C., 1991: A three-dimensional generalization of Eliassen's balanced vortex equations derived from Hamilton's principle. *Quart. J. Roy. Meteor. Soc.*, **117,** 435–448.

Davies-Jones, R., 1991: The frontogenetical forcing of secondary circulations. Part I: The duality and generalization of the Q vector. *J. Atmos. Sci.*, **48,** 497–509.

DeMaria, M., J.-J. Baik, and J. Kaplan, 1993: Upper-level eddy angular momentum fluxes and tropical cyclone intensity change. *J. Atmos. Sci.*, **50,** 1133–1147.

Eliassen, A., 1952: Slow thermally or frictionally controlled meridional circulation in a circular vortex. *Astrophys. Norv.*, **5,** 19–60.

Emanuel, K. A., 1989: The finite-amplitude nature of tropical cyclogenesis. *J. Atmos. Sci.*, **46,** 3431–3456.

Holland, G. J., 1983: Angular momentum transports in tropical cyclones. *Quart. J. Roy. Meteor. Soc.*, **109,** 187–210.

Molinari, J., 1993: Environmental controls on eye wall cycles and intensity change in Hurricane Allen (1980). *Proc. ICSU/WMO Int. Symp. on Tropical Cyclone Disasters,* Beijing, China, World Meteorological Society, in press. [Available from the author at Department of Atmospheric Science, ES-225, State University of New York at Albany, 1400 Washington Avenue, Albany, NY 12222.]

——, and D. Vollaro, 1989: External influences on hurricane intensity. Part I: Outflow layer eddy angular momentum fluxes. *J. Atmos. Sci.*, **46,** 1093–1105.

——, and ——, 1990: External influences on hurricane intensity. Part II. Vertical structure and response of the hurricane vortex. *J. Atmos. Sci.*, **47,** 1902–1918.

——, ——, and F. Robasky, 1992: Use of ECMWF operational analyses for studies of the tropical cyclone environment. *Meteor. Atmos. Phys.*, **47,** 127–144.

Montgomery, M. T., and B. F. Farrell, 1993: Tropical cyclone formation. *J. Atmos. Sci.*, **50,** 285–310.

Ooyama, K., 1969: Numerical simulation of the life cycle of tropical cyclones. *J. Atmos. Sci.*, **26,** 3–40.

——, 1982: Conceptual evolution of theory and modeling of the tropical cyclone. *J. Meteor. Soc. Jap.*, **60,** 369–379.

Pfeffer, R. L., and M. Challa, 1981: A numerical study of the role of eddy fluxes of momentum in the development of Atlantic hurricanes. *J. Atmos. Sci.*, **38,** 2393–2398.

Raymond, D. J., 1992: Nonlinear balance and potential vorticity thinking at large Rossby number. *Quart. J. Roy. Meteor. Soc.*, **118,** 987–1016.

Schubert, W. H., and J. J. Hack, 1983: Transformed Eliassen balanced vortex model. *J. Atmos. Sci.*, **40,** 1571–1583.

Shapiro, L. J., and H. E. Willoughby, 1982: The response of balanced hurricanes to local sources of heat and momentum. *J. Atmos. Sci.*, **39,** 378–394.

Skubis, S., and J. Molinari, 1987: Angular momentum variation in a translating cyclone. *Quart. J. Roy. Meteor. Soc.*, **113,** 1041–1048.

Smith, R. K., 1981: The cyclostrophic adjustment of vortices with application to tropical cyclone modification. *J. Atmos. Sci.*, **38,** 2021–2030.

Sundqvist, H., 1970: Numerical simulations of the development of tropical cyclones with a ten-level model. Part 1. *Tellus,* **22,** 359–390.

Willoughby, H. E., 1979: Forced secondary circulations in hurricanes. *J. Geophys. Res.*, **84,** 3173–3183.